Biophysical Chemistry 7 (1977) 193–204

DIELECTRIC STUDIES ON SELF-ASSOCIATING NUCLEOSIDES AND BASES IN AQUEOUS SOLUTION

J.C.W. SHEPHERD and G. SCHWARZ
Department of Biophysical Chemistry, Biocentre of the University of Basel, 4056 Basel, Switzerland

Received 15 March 1977

Measurements have been made of the dielectric properties of aqueous solutions in which aggregates are formed by stacking. The nucleosides cytidine, uridine and thymidine, and the bases purine, pyrimidine and 6-methylamino-9-methylpurine (N^6,N^9-dimethyladenine) were investigated at around 1 MHz, where the static increments can be determined, and for cytidine, dimethyladenine, uridine and pyrimidine measurements were also made in the 100–2000 MHz range where the main relaxation of the solute dipoles is found. Whereas cytidine and purine show a positive static dielectric increment increasing linearly with concentration, dimethyladenine, uridine, thymidine and pyrimidine show a similar negative effect. Also, within the experimental accuracy, single relaxation times are found for the solute dispersions investigated.

It is suggested that these relaxations correspond to the effects of free rotation of individual polar molecules in the plane of stacking. This phenomenon would also account for the linear variation of the dielectric increments with concentration. These increments are thought to be positive or negative due to the varying balance in the solutions between the loss of polarization due to displaced and "bound" water and the corresponding gain due to the polarity of the solute molecules.

1. Introduction

Experimental studies of the self-association of a number of nucleosides and bases in aqueous solution have been made by methods such as vapour pressure osmometry, sedimentation equilibrium, optical or NMR measurements (see e.g. [1–4]). The molecules are thought to stack to a varying degree and the corresponding thermodynamic parameters have been deduced (see [5] for a survey). In the case of dimethyladenine the kinetics of the interactions have also been investigated by means of ultrasonic absorption techniques [6]. The dipole moments of some of these molecules have been calculated and some have been measured in non-aqueous solutions (see e.g. [5,7,8]). However, it would appear that no dielectric measurements have as yet been made in aqueous solutions and therefore the present work has been undertaken in order to reveal some of the main experimental phenomena, which should prove of interest with regard to the nature of the stacking interactions. The measurements have been restricted in the first case to bases and nucleosides which are reasonably soluble in water, and nucleotide solutions with their higher conductivity have been avoided.

2. Materials and experimental methods

All test substances were of analytical grade, the 6-methylamino-9-methylpurine (dimethyladenosine) being from the Cyclo Chemical Co. and the other nucleosides and bases from Merck, Serva and Koch-Light. The solutions were made up with bidistilled water of low conductivity ($\approx 10^{-6}\ \Omega^{-1}\ cm^{-1}$).

In the 200 kHz–5 MHz range the experimental cell consisted of two concentric platinum electrodes with teflon insulation and teflon thread used for sealing the screw joints. Measurements of capacity and conductance were made using a Wayne Kerr type B201 transformer ratio arm bridge with a Hewlett Packard type 651B test oscillator as source and a Rohde and Schwarz type USVH selective microvoltmeter as detector. Details of the measuring method have previously been given [9], and in this case water was used as a standard of comparison for the given solutions.

Using the same experimental cell, some measurements were also made in the 1–50 kHz range, with a Wayne Kerr B221 bridge, a Hewlett Packard 200 CD oscillator and a Rohde and Schwarz tunable indicating amplifier type UBM.

For the higher frequency measurements (100–2000 MHz (a coaxial line cell has been constructed similar in design to one already described [10], but with a number of modifications, including a somewhat smaller inner diameter of the cell (1.0 cm instead of 1.5 cm) in order to reduce the propagation of higher modes, an improved ease of movement of the probe-carrying inner conductor (as derived by installing two ball-races, and an electronic digital measurement of the probe position attained by incorporating a TESA gauge. Thermostatic control was achieved to within 0.1°C by means of passing water (or alcohol at 0°C) through an outer jacket on the cell. The coaxial line measuring methods have also been detailed elsewhere [10].

3. Results

The first measurements were made at 200 kHz, 1 MHz and 5 MHz on cytidine solutions at various concentrations up to the solubility limit of ≈0.75 M. At any given concentration the permittivity appeared approximately constant with respect to frequency, thus indicating that dispersion occurred at much higher frequencies. (No dispersion at lower frequencies could be detected.) Since cytidine was known to associate considerably at such concentrations [2,3], the almost exactly linear variation of increment with concentration as shown at 1 MHz and 20°C in fig. 1 was interesting (linearity was established well within the estimated maximum experimental error of 0.3% in ϵ' for the solution) in view of non-linear effects which might be expected from the known aggregation of such polar molecules. The effect of varying the aggregation by altering the temperature was therefore tried (see fig. 2) but the proportionality of increment to concentration remained at all temperatures to within the experimental errors (which are somewhat higher at 40° and 50°C due to increased conductivity of the solutions). The static permittivity was also found to vary linearly with $1/T$ as for non-aggregating solutes.

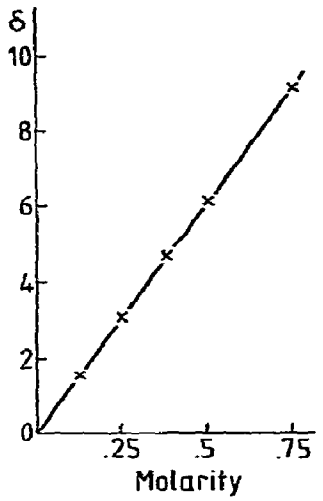

Fig. 1. Variation of static dielectric increment δ with concentration for cytidine solution, as measured at 1 MHz and 20°C.

To gather further information with regard to the polarization mechanism involved, measurements were now made at 100–2000 MHz and at temperatures from 0° to 40°C on a 0.5 M cytidine solution. This concentration was chosen so that the incremental changes above and below the permittivity of water were sufficiently large to be reasonably accurately measured. Greater concentrations were avoided since

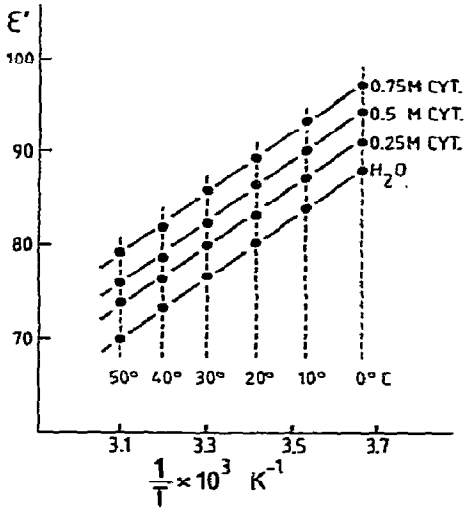

Fig. 2. Variation of static permittivity with temperature for various cytidine solutions.

even for non-aggregating highly polar solutes in aqueous solution the relaxation time has then been found to start to increase with concentration [11].

The dispersion region of the cytidine was clearly revealed at all temperatures (illustrated at 20°C in fig. 3). Within the estimated experimental errors (1.5% in ϵ' and 3% in ϵ'') an analysis has been possible in all cases in terms of two Debye dispersions: (1) for the solute and (2) for the water of solution. The permittivity ϵ' and loss factor ϵ'' could be expressed in the form

$$\epsilon' = \epsilon_\infty + \frac{A_1}{1+(\omega\tau_1)^2} + \frac{A_2}{1+(\omega\tau_2)^2}, \quad (1)$$

$$\epsilon'' = \frac{(\omega\tau_1)A_1}{1+(\omega\tau_1)^2} + \frac{(\omega\tau_2)A_2}{1+(\omega\tau_2)^2}, \quad (2)$$

where ω is the angular frequency of measurement, A_1 and A_2 are amplitude factors, and τ_1 and τ_2 the respective relaxation times. ϵ_∞ is the permittivity of the solution at frequencies much higher than the relaxation frequencies f_1 and f_2 and to a reasonable approximation could be clamped at 4.5, thus approximating to the high frequency permittivity of water.

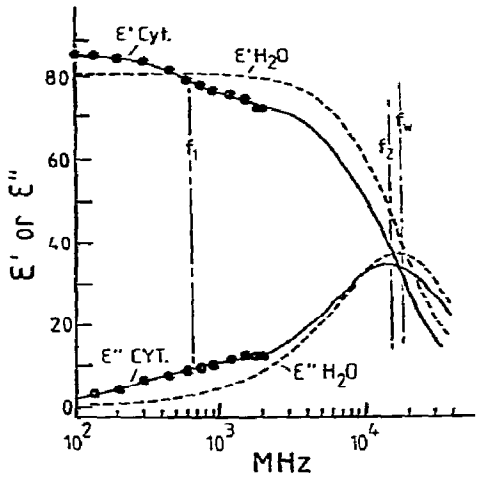

Fig. 3. Dispersion of 0.5 M cytidine solution shown relative to that of pure water, both measured at 20°C. f_1 (628 MHz) is the relaxation frequency of cytidine in solution, f_2 (14780 MHz) that of the water of solution and f_w (17340 MHz) that of pure water. (The continuous lines are the fitted curves.)

The values of the parameters obtained from the least squares analysis are shown in table 1, together with their estimated 95% confidence intervals, and will be discussed in detail later.

Table 1
Parameters obtained by fitting the measured dispersions

	A_1	τ_1 (ps)	f_1 (MHz)	A_2	τ_2 (ps)	f_2 (MHz)
0.5 M cytidine						
0°C	13.1 ± 1.0	488 ± 66	326	74.8 ± 0.7	20.1 ± 1.4	7930
10°C	13.2 ± 0.7	363 ± 39	438	72.4 ± 0.5	14.7 ± 1.1	10820
20°C	13.0 ± 0.6	253 ± 21	628	68.1 ± 0.4	10.8 ± 1.0	14780
30°C	10.7 ± 0.5	214 ± 21	743	66.9 ± 0.4	9.9 ± 0.9	16040
40°C	11.1 ± 0.6	157 ± 17	1016	62.9 ± 0.5	7.1 ± 0.1	22430
0.5 M dimethyladenosine						
0°C	2.2 ± 0.8	577 ± 278	276	76.5 ± 0.5	20.6 ± 1.0	7730
20°C	2.9 ± 0.7	370 ± 132	430	69.5 ± 0.5	10.4 ± 1.0	15340
40°C	2.4 ± 0.4	202 ± 63	786	63.0 ± 0.4	6.1 ± 0.8	26070
0.6 M uridine						
20°C	5.2 ± 0.8	171 ± 44	930	66.6 ± 0.6	10.6 ± 1.4	14940
0.9 M uridine						
20°C	7.1 ± 0.7	264 ± 42	603	63 ± 0.5	12.4 ± 1.0	12840
0.5 M cytidine in D_2O						
20°C	12.5 ± 0.6	283 ± 30	563	67.6 ± 0.5	13.7 ± 1.1	11590

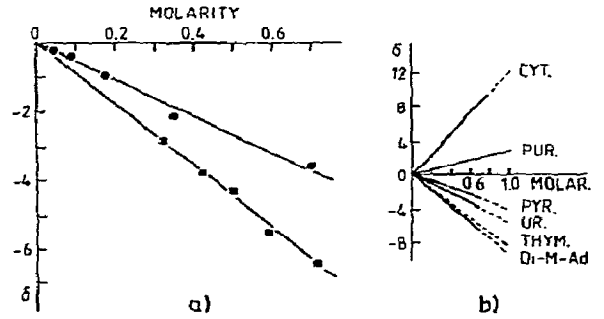

Fig. 4. (a) Negative dielectric increments of uridine (•) and dimethyladenine (▪), measured at 1 MHz and 20°C. (b) Comparison of positive and negative increments shown by cytidine, purine, pyrimidine, uridine, thymidine and dimethyladenine (1 MHz, 20°C).

Attention now turned to the behaviour of other nucleosides and bases. In contrast to cytidine, uridine and dimethyladenine were found to have negative dielectric increments (1 MHz, 20°C) showing also a linear variation with concentration within the measuring accuracy (see fig. 4a). Exploratory work with pyrimidine, thymidine and purine, showed that the first two substances had similar negative increments but that purine had a positive increment (see fig. 4b giving the relative behaviour of all substances investigated).

With regard to the dielectric dispersions observed, that for 0.6 M uridine solution at 20°C is shown in fig. 5. (Some ϵ' values for a 0.5 M pyrimidine solution are also shown on this figure. This smaller molecule

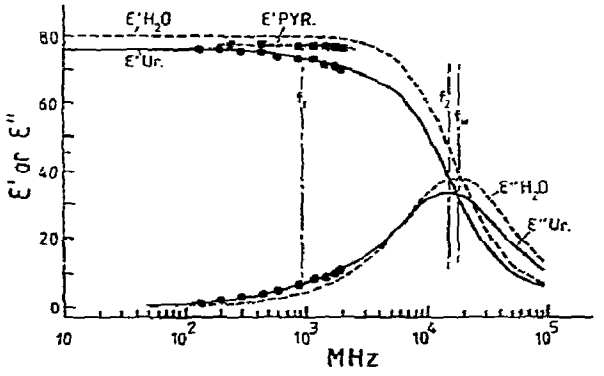

Fig. 5. Dispersions of 0.6 M uridine solution and water at 20°C. With notation as in fig. 3, f_1 = 930 MHz and f_2 = 14940 MHz. Measurements of ϵ' for a 0.6 M pyrimidine solution are also shown.

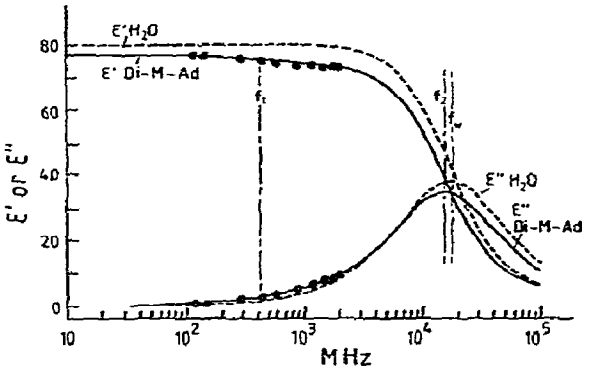

Fig. 6. Dispersions of 0.5 M dimethyladenine and water at 20°C. f_1 = 430 MHz, f_2 = 15340 MHz.

(molecular weight 80.1) has hardly started its dispersion at 2000 MHz.) The behaviour of 0.5 M dimethyladenine at 20°C is given in fig. 6 and has also been observed at 0° and 40°C. Fits could again be obtained to these curves in terms of two Debye dispersions and the parameters deduced are also shown in table 1.

Additional measurements on a 0.9 M uridine solution (see table 1) showed that the relaxation frequency of the solute dispersion was lowered from 930 to 600 MHz (which may be partly due to the above mentioned concentration effect [cf. 11] and partly to greater aggregation). The change produced by using D_2O instead of water as the solvent was also investigated for a 0.5 M cytidine solution (table 1). The amplitude A_1 and the relaxation time τ_1 for the cytidine dispersion were hardly altered, whereas the relaxation time τ_2 has lengthened approximately in the ratio (1.3 : 1) of the relaxation times D_2O/H_2O at this temperature.

Considering the 95% confidence intervals given on the parameters in table 1, it is noted that the relaxation time τ_1 for the solute is less well determined in the case of uridine and dimethyladenine than for cytidine and the proportional error in A_1 is smaller for the latter. This is to be expected since the dispersions of uridine and dimethyladenine have smaller amplitudes and are less accurately determined as superimposed on the large dispersion of water. The 95% confidence levels are however a generous error estimation (≈±2 standard deviations) and the linear relations with τ_1 later found (see figs. 9 and 10) indicate that the accuracy actually achieved is well within these limits.

4. Discussion

4.1. Static increments

The fact that positive and negative increments have been observed may first be considered in relation to fig. 7, a schematic representation of the dispersions (showing them as if they were well separated; in fact they overlap). δ, the static increment ($\delta = A_1 - D$) may be taken to be a combination of two effects, D the decrement caused by displacing water by the solute and A_1 the positive increment due to the solute polarization. D is given approximately by

$$D = \frac{Mc\bar{v}}{1000}(\epsilon_{sw} - \epsilon_{\infty s}), \qquad (3)$$

where M is the molecular weight of the solute molecule, c its concentration in moles/litre and $\bar{v}$ its partial specific volume. ϵ_{sw} is the static permittivity of water and $\epsilon_{\infty s}$ the high frequency permittivity of the solute. To the degree of approximation considered, $\bar{v}$ can be regarded as constant and thus D can be expected to be proportional to concentration. Since the total effect δ has been found experimentally to have such a proportionality, A_1 should also vary similarly.

At this point it would seem appropriate to estimate

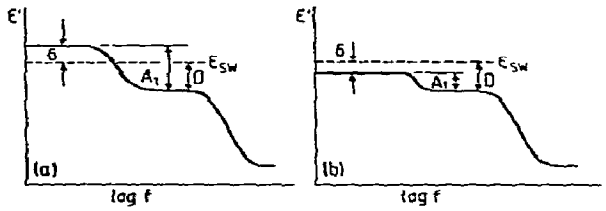

Fig. 7. (a) Positive increment δ when $A_1 > D$. (b) Negative increment δ when $A_1 < D$. (ϵ_{sw} is static permittivity of water).

Table 3
Mean aggregation numbers m (including monomers in average)

Temp (°C)	0.6 M Ur.	0.5 M Cyt.	0.5 M Di-M-Ad.
0	1.40	1.47	9.9
10		1.40	
20	1.30	1.35	6.0
30		1.31	
40	1.24	1.27	3.9

the degree of aggregation in the solutions where the dispersion has been measured. This may be deduced on the assumption of an isodesmic model, which has been found to concord with observed data [cf. 3–6]. The variation of the association constant K with temperature is shown in table 2 (deduced from the thermodynamic parameters given in [5]) and the mean aggregation numbers at various temperatures derived for 0.6 M uridine, 0.5 M cytidine and 0.5 M dimethyladenine (table 3).

For these solutions of high permittivity, the amplitude A_1 can be shown to be proportional to $\Sigma_a N_a \mu_a^2$, where N_a is the number of any particular species of rotating polar unit per unit volume and μ_a is its dipole moment [12]. Since any such solution contains a mixture of monomers and various types of aggregates, it must be considered how such a linear relation between A_1 and concentration can arise. An aggregation model as shown in fig. 8 is proposed, in which i nucleosides stack with their bases parallel to each other and perpendicular to the axis n. It is assumed that the dipole moments μ of the nucleosides lie in the plane of the bases (which may be a reasonable approximation, cf. [8]) and that no appreciable component lies along the axis n.

Table 2
Values of association constant K (M^{-1})

	Temperature (°C)				
	0	10	20	30	40
uridine	0.95		0.67		0.50
cytidine	1.37	1.13	0.95	0.81	0.69
dimethyladenosine	177		59		23

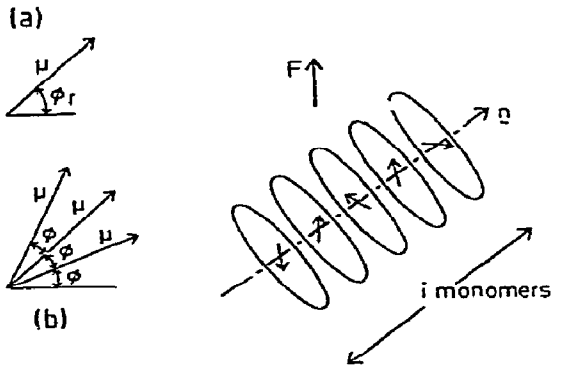

Fig. 8. Aggregation model, in which the monomer dipole moments μ are in the plane of stacking and at right angles to the axis n.

Three possibilities are now considered:

(a) The monomers may aggregate rigidly together, but with their dipoles randomly oriented in the stacking plane. Referring to fig. 8a, if N_i is the number of monomers per unit volume in all aggregates of i monomers, then the contribution to $\Sigma N_a \mu_a^2$ is

$$\frac{\mu^2}{(2\pi)^i}\left(\frac{N_i}{i}\right)\int_0^{2\pi}\cdots\int_0^{2\pi}\left\{\left(\sum_r^{1,i}\cos\phi_r\right)^2+\left(\sum_r^{1,i}\sin\phi_r\right)^2\right\}\mathrm{d}\theta_1\,\mathrm{d}\theta_2\ldots\mathrm{d}\theta_i = N_i\mu^2.$$

Thus, summing over all types of aggregates, the final contribution to A_1 is proportional to $N_t\mu^2$, where N_t is the total number of monomers in the solution. Hence A_1 will be proportional to the weighed-in concentration of monomers, as found experimentally.

(b) The monomers aggregate rigidly together, but with a fixed geometry between neighbours. In this case it is difficult to see how the simple linearity of A_1 can be explained. For example, if a constant angle ϕ is assumed between successive dipoles (see fig. 8b), then it is found that the contribution to A_1 from all aggregates containing i monomers is proportional to

$$\frac{1-\cos i\phi}{i(1-\cos\phi)}N_i\mu^2$$

and not simply to $N_i\mu^2$ as before. A particular geometry of aggregation (for example, dimers with each dipole at around 90° to its neighbour) might favour linearity, but that this geometry should occur with so many differing molecules is hard to imagine.

(c) The monomers stack together as before, but each monomer can rotate freely about the axis n. This possibility is treated in detail for not only can it explain the linearity of A_1 with concentration but it will be found to give a more convincing explanation of the observed relaxation times than the hypothesis (a). A theory of Budó ([13]; also see appendix) shows for this non-rigid association model that the static polarization P is given by

$$P = (N_t\mu^2/3kT)F_0, \tag{4}$$

where N_t is again the total number of nucleosides or bases (from all species of aggregates including monomers) per unit volume, F_0 the internal directing field and the other symbols have their usual significance. Hence, as for solutions of highly polar non-aggregating molecules, the following relation between A_1 and μ can be derived [12]

$$g^{1/2}\mu = 10^{18}(1000\,kT/2\pi N_A)^{1/2}(A_1/c)^{1/2} \quad \text{Debye}, \tag{5}$$

where g is Kirkwood's correlation factor, c the weighed-in concentration of solute in moles/litre, N_A Avogadro's number and kT is inserted in erg ($g^{1/2}\mu \simeq 3.27\,A_1^{1/2}$ Debye at 20°C for c = 1 mole/litre).

Thus, in spite of the aggregation, it is seen for models (a) and (c) that A_1 is proportional to concentration, in accordance with the present observations.

4.2. Relaxation times

As already indicated, model (c) is capable of an adequate explanation of the measured relaxation times, whereas model (a) fails in this respect. For an alternating directing field $F_0\exp(j\omega t)$, the free-rotation theory shows (see appendix) that the polarization P_i produced by the aggregates containing i bases is given by

$$P_i = \frac{N_i\mu^2F_0\exp(j\omega t)}{3kT(1+j\omega\tau_i)}, \tag{6}$$

where

$$1/\tau_i = D_n + D_i = kT(1/\rho_n + 1/\rho_i) \tag{7}$$

and N_i is the overall number of monomers per unit volume in these i-fold aggregates. D_n is the rotational diffusion coefficient for any one monomer to rotate independently about the axis n (fig. 8) and D_i the coefficient for the whole aggregate to turn about an axis perpendicular to n. ρ_n and ρ_i are the corresponding frictional coefficients.

Assuming that all the polarizations P_i and that of the water $P_{(2)}$ are additive, a mixture theory for the alternating field case can be developed [cf. 12] as an extension of the method applied for static fields to highly polar solutions. This yields for the complex dielectric constant ϵ^*

$$\epsilon^* - \epsilon_\infty = \sum_i \frac{(A_1)_i}{1 + j\omega\tau_i} + \frac{A_2}{1 + j\omega\tau_2}, \qquad (8)$$

where the $(A_1)_i$ values are related by eq. (5) to the total concentration c_i of monomers in each type of aggregate.

Thus the form of analysis used (eqs. (1) and (2)) has been justified. With the present experimental accuracy, however, only one relaxation time could be detected for the solute dispersion. This is reasonable since: (a) in the case of dimethyladenine ($m = 6$ at 20°C) $D_i \ll D_n$ and $1/\tau_i \doteq D_n$ from eq. (7) for all species of elongated aggregates present; (b) for cytidine and uridine most of the nucleosides can be shown to be in the form of monomers with roughly half this number as dimers and the resulting distribution of relaxation times has been too small to be detected.

Table 4 shows a comparison between the estimated values of τ_1 on the basis of this theory and those actually observed. As a first working hypothesis the nucleosides have been considered as spheres of equal volume V, and hence $\rho_n = 8\pi\eta a^3$ where a is the effective radius or $\rho_n = 6V\eta$ (η has been taken as the viscosity of water and V has been deduced from measured values of the partial specific volume). Now, when calculating τ_1 from eq. (7), ρ_i has been taken to be $m\rho_n$ for cytidine and uridine and, in the case of dimethyladenine $1/\rho_i$ has been regarded as negligible.

For cytidine, the temperature variation of m is relatively small (see table 3) and can be expected to have little effect on τ_1 ($\doteq 6V\eta/kT(1 + 1/m)$). In the case of dimethyladenine, although m varies considerably, τ_1 is not appreciably affected since $D_i \ll D_n$. In both cases, therefore, the usual linear plots of $T\tau$ versus η passing through the origin would be expected and are in fact obtained (fig. 9). These graphs together with the data in table 4 thus indicate a reasonable correspondence between the computed and observed relaxation times.

If random fixed aggregation (a) is supposed, however, and if it is further assumed that the rigid aggregate is an elongated ellipsoid of revolution with axial ratio a/b ($a > b$) and with its resultant dipole moment at right angles to the major axis, the theory of Perrin [14] shows that τ increases very considerably for larger aggregates ($\tau \doteq 7\tau_0$ for $a/b = 5$, where τ_0 is the relaxation time corresponding to single monomers). Thus, with the very wide distribution of aggregates in dimethyladenine, one would certainly expect a considerable spread of relaxation times and a mean relaxation time in excess of that observed. In fact, on

Table 4
Comparison of measured relaxation times τ_1 at 20°C and those estimated on basis of free rotation model (c)

	Mol. wt.	Partial specific volume (ml/g)	Molar volume (ml)	Mean aggreg. no. m	$\tau_1 \doteq \frac{6V}{kT(1 + 1/m)}$	τ_1 calc. (ps)	τ_1 measured (ps)
0.5 M Cyt.	243.2	0.63	153.2	1.35	$\frac{3.45\,V\eta}{kT}$	216	253 ± 21
0.5 M Di-M-Ad.	163.2	0.73	119.1	6.0	$\frac{6\,V\eta}{kT}$	294	370 ± 132
0.6 M Ur.	244.2	0.62	151.6	1.30	$\frac{3.39\,V\eta}{kT}$	211	171 ± 44

the basis of Perrin's theory and using the mean aggregation numbers in table 3, relaxation times of 3830, 1260 and 530 ps are estimated at 0°, 20° and 40°C, whereas 577, 370 and 202 ps, respectively, were observed (table 1). The corresponding values deduced from the free rotation theory (c), 565, 294 and 180 ps, thus give much better agreement with the present measurements.

4.3. Activation enthalpies

By considering dielectric relaxation as a rate process and assuming that the Eyring equation

$$\tau_1 = \frac{h}{kT}\exp(\Delta G^{\ddagger}/RT)$$

$$= \frac{h}{kT}\exp(-\Delta S^{\ddagger}/R)\exp(\Delta H^{\ddagger}/RT),$$

is applicable and that $\Delta S^{\ddagger}$ and $\Delta H^{\ddagger}$ are independent of temperature, a linear plot of $\ln(T\tau_1)$ versus $1/T$ is normally obtained in the case of individually rotating monomers. As in the case of the variation of $T\tau_1$ with η above, the changes in m with temperature for cytidine and dimethyladenine can be expected to have little effect on the linearity of these rate process graphs (model (c) now assumed). They are shown in fig. 9 and an activation enthalpy of ≈4.3 kcal/mole is deduced in both cases. This is a value commonly found for relaxations in aqueous solutions, and is taken to indicate the breaking of a hydrogen bond as the rate limiting step in these processes.

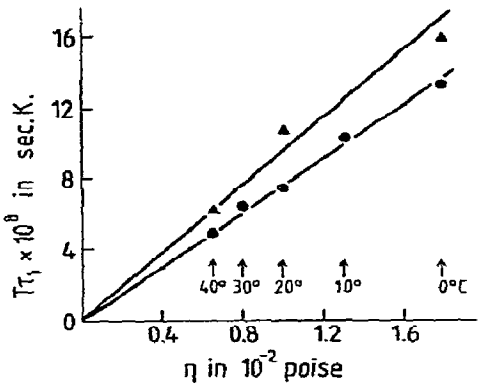

Fig. 9. Plots of $T\tau_1$ against $1/T$: • cytidine, ▲ dimethyladenine.

4.4. Dipole moments and bound water

It is also interesting to deduce from the two component analyses (table 1) the values of the decrement D (cf. fig. 7). These are shown in table 5 and it is noted that these decrements are on the whole greater than the decrease in ϵ' due to displaced water (as deduced approximately from the partial molar volume at 20°C using eq. (3) and taking $\epsilon_{\infty s} \doteq \epsilon_{\infty w}$). This would indicate that some of the neighbouring water is either bound to the nucleoside or that its structure has been so affected that it has a lower permittivity at intermediate frequencies, where the solute has already relaxed but the pure water dispersion has not started.

A similar conclusion may also be reached by considering the effective dipole moments $g^{1/2}\mu$ in solution of the nucleosides, as deduced from the amplitude A_1 of the solute dispersion and eq. (5). These are shown in table 6 together with the errors corresponding to the 95% confidence limits in A_1 (it should be noted that there is additional uncertainty introduced by using a theory applicable to point dipoles and neglecting a more detailed consideration of molecular shape and charge distribution). It is seen that the values are considerably greater than the dipole moments previously calculated or as measured in non-aqueous solutions. Some indication is therefore given either that some bound water rotates with the nucleoside, thus increasing its moment, or that the Kirkwood correlation factor g between nucleoside and neighbouring water is high.

The relaxation time τ_2 for the water of solution has proved in all cases to be somewhat larger than that for pure water. This fact is illustrated in fig. 10, where the plots of $\ln(T\tau_2)$ against $1/T$ for cytidine and dimethyladenine solutions are shown. The line for cytidine's water of solution is approximately parallel to that for pure water (but displaced to larger values of τ_2) and both give an activation enthalpy of ≈3.8 kcal/mole. The line for the water of solution in dimethyladenine solution has a slightly greater slope and is also similarly displaced. One explanation for this lengthening of τ_2 could again be that some water molecules near the solute have a longer relaxation time than that in free water.

Table 5
Comparison of measured decrements ($D = \epsilon_{SW} - \epsilon_{\infty A} - A_2$) and those deduced from eq. (3)

	Measured D					D calculated from $\bar{v}$ at 20°C
Temp. (°C)	*0*	*10*	*20*	*30*	*40*	
0.5 M Cyt.	8.4	6.9	7.7	5.2	5.8	5.7
0.5 M Di-M-Ad.	6.7		6.3		5.1	4.5
0.6 M Ur.			9.2			6.8

Table 6
Comparison of dipole moments (cytidine and uridine are thought to be predominantly in the anti form; cf. [7,8])

Solution measured	Temp. (°C)	Effective dipole moment $g^{1/2}\mu$ (Debye)	μ otherwise calculated or measured (Debye)
0.5 M cytidine in H_2O	0	16.2 ± 0.6	8.8 for anti conformer [a]
	10	16.5 ± 0.4	6.7 for syn conformer [a]
	20	16.7 ± 0.4	
	30	15.4 ± 0.4	
	40	15.9 ± 0.4	
0.5 M cytidine in D_2O		16.4 ± 0.4	
0.5 M dimethyladenosine in H_2O	0	6.6 ± 1.1	2.8 for 9-methyladenine [b]
	20	7.9 ± 0.9	3,0 for 9-n-butyladenine [c]
	40	7.4 ± 0.6	
0.6 M uridine in H_2O	20	9.6 ± 0.7	7.0 for anti conformer [a]
0.9 M uridine in H_2O	20	9.2 ± 0.5	3.4 for syn conformer [a]

[a] Calculated [8]. [b] Calculated [15]. [c] Measured in CCl_4 [15].

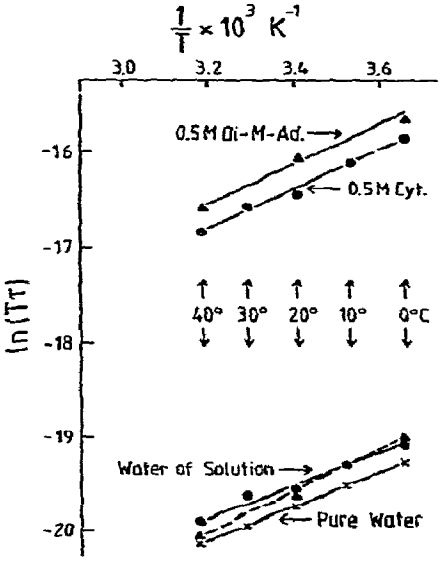

Fig. 10. Plots of $\ln(T\tau)$ against $1/T$: ● cytidine, ▲ dimethyladenine.

4.5. Additional remarks

It is wise to stress the tentative nature of the present interpretation of the experimental data. No doubt there are some steric hindrances to free rotation within the stacks in particular instances and Budó has later shown [16] that in this case specific assumptions with regard to an intermolecular potential have then to be made in order to deduce the dielectric properties. Without information on such potentials, it is difficult to foresee the dielectric effects except in so far as to anticipate that simple linearity of increment with concentration and narrow

distributions of relaxation times seem unlikely to be attained if the hindrance is considerable.

From the rate constant for dissociation, for example 6.6×10^7 s^{-1} at 40°C for dimethyladenine [6], the mean time for which two neighbouring bases are associated is approximately 1.5×10^{-8} s. Thus, since the measured dielectric relaxation time is $\sim 2 \times 10^{-10}$ s at this temperature, there is ample time for rotational movements of the individual molecules relative to each other to occur in an aggregate of m monomers before it dissociates at any of the $(m-1)$ possible sites. It is considered that two aggregating bases may well slightly separate several times before finally the surface of the water cavity round them is broken and they dissociate (cf. the reaction scheme given for dissociation in [6] and the theory of Sinanoğlu and Abdulnar [17] which proposes that one main factor promoting stacking is the decrease of water surface area round the bases). During such separations it might well be that rotational move ment within a stack is facilitated.

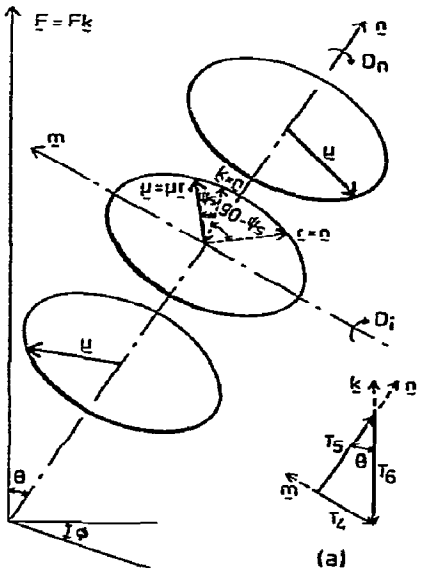

Fig. 11. Illustrating an aggregate of i molecules, each with dipole μ rotating independently about the axis n and in a plane perpendicular to n.

Acknowledgement

We wish to thank Dr. M.P. Heyn for stimulating discussion and Mr. A. Lustig for measuring the partial specific volumes.

Appendix

Dielectric polarization due to molecules with freely rotating groups has been treated by Budó [13]. However, his original article is not easily accessible and also more complicated than would be necessary in this case. Since the theory is crucial for the present interpretation of dielectric data a brief derivation of eqs. (4), (6) will be given.

The directions of stacks and dipoles are described in fig. 11. The unit vector n is normal to the stacking plane and simultaneously represents the axis of free rotation of individual stacked molecules. The direction of n is to be expressed in terms of the conventional spherical coordinates θ, ϕ where $\theta = 0$ indicates the directing field, $F = Fk$. The unit vector r of a dipole moment in a stacked molecule is perpendicular to n and makes an angle ψ_s with the vector $k \times n$. Since the moment of any dipole in the direction of the field will always be independent of ϕ, rotational symmetry with respect to this angle can be assumed.

Aggregates consisting of i stacked molecules are now considered. The number of such particles which at time t fall in the domain $d\Omega = 2\pi \sin\theta \, d\theta \, d\psi_1 \ldots d\psi_i$ is to be written as

$$dN_i = N_i \gamma_i(\theta, \psi_1, \psi_2, \ldots, \psi_i, t) \, d\Omega$$

thus introducing a respective distribution function γ_i. From the normalization relation

$$\int_0^{\pi} \int_0^{2\pi} \ldots \int_0^{2\pi} \gamma_i \, d\Omega = 1 \qquad \text{(A1)}$$

it follows for statistically random orientation

$$\gamma_i^0 = 1/(2(2\pi)^{i+1}). \qquad \text{(A2)}$$

The total dielectric polarization (dipole moment per unit volume) of all these aggregates must be parallel to F and its magnitude can be generally calculated as

$$P_i = 2\pi N_i \mu \int_0^{\pi} \int_0^{2\pi} \cdots \int_0^{2\pi} \gamma_i \sin^2\theta \times \sum_s^{1,i} \sin\psi_s \, d\theta \, d\psi_1 \ldots d\psi_i \qquad (A3)$$

(note that the individual dipole component is $\mu \sin\theta \sin\psi_s$).

For a static field F_0 a Boltzmann distribution must occur at equilibrium and

$$\bar{\gamma}_i = A \exp(\alpha_0 \sin\theta \, \Sigma_s \sin\psi_s), \qquad (A4)$$

where $\alpha_0 = \mu F_0/kT$ and the constant A can be determined from the normalization equation (A1). In the present experiments $\alpha_0 \ll 1$ and

$$\bar{\gamma}_i = \gamma_i^0(1 + \alpha_0 \sin\theta \, \Sigma_s \sin\psi_s). \qquad (A5)$$

(A3) now yields

$$\bar{P}_i = (N_i\mu^2/3kT)F_0 \qquad (A6)$$

or the total static polarization P for all species is given by

$$P = \frac{\Sigma N_i \mu^2}{3kT} F_0 = \frac{N_t \mu^2}{3kT} F_0 \qquad (A7)$$

giving eq. (4) in the text.

In order to evaluate the dielectric relaxation of the present system the time dependence of γ_i has to be determined. A relevant approach takes advantage of the equation of continuity which results from the fact that the increase of the number of aggregates in a certain domain is equal to the net influx. The latter results from the action of the torque exerted by the field on the dipoles and the counteraction of rotational diffusion. Any changes in chemical equilibrium produced by the field and consequent changes of γ_i [18] can be neglected since the chemical rate process of stacking is sufficiently slow compared with the rotational rate [6,19].

The net influx into $d\Omega$ caused by the field is

$$-\frac{1}{\sin\theta}\left\{\frac{\partial}{\partial\theta}\left(\sin\theta \cdot j_\theta\right) + \sum_s \frac{\partial}{\partial\psi_s}\left(\sin\theta \cdot j_s\right)\right\} d\Omega = (\partial\gamma_i/\partial t)_F d\Omega, \qquad (A8)$$

where the flux densities

$$j_\theta = \gamma_i(d\theta/dt)_F, \qquad j_s = \gamma_i(d\psi_s/dt)_F \qquad (A9)$$

involve the respective field induced angular velocities. To determine $(d\theta/dt)_F$ and $(d\psi_s/dt)_F$, the field F is resolved (see fig. 11) into its components $(F\cos\theta)\boldsymbol{n}$ and $(F\sin\theta)\boldsymbol{m}$ parallel and perpendicular to $\boldsymbol{n}$ ($\boldsymbol{m}$ is a unit vector normal to $\boldsymbol{n}$ in the plane containing $\boldsymbol{k}$ and $\boldsymbol{n}$, i.e. $\boldsymbol{m} = \boldsymbol{n} \times (\boldsymbol{k} \times \boldsymbol{n})/\sin\theta$. The torque T_1 of $(F\sin\theta)\boldsymbol{m}$ on the dipole $\mu\boldsymbol{r}$ is $(\mu F \sin\theta)\boldsymbol{r} \times \boldsymbol{m}$ or $(\mu F \sin\theta\cos\psi_s)\boldsymbol{n}$. With the present assumptions this acts on the single molecule s and gives it an angular velocity about $\boldsymbol{n}$ (diffusional constant D_n)

$$(d\psi_s/dt)_F = (D_n \alpha \sin\theta \cos\psi_s)n, \qquad (A10)$$

where $\alpha = \mu F/kT$. On the other hand the torque T_2 of $(F\cos\theta)\boldsymbol{n}$ on the dipole $\mu\boldsymbol{r}$ is $(\mu F\cos\theta)\boldsymbol{r} \times \boldsymbol{n}$ and acts on the whole aggregate, turning it about an axis perpendicular to $\boldsymbol{n}$ (diffusional constant D_i). T_2 can be resolved into two components $(\mu F\cos\theta\sin\psi_s)$ $\boldsymbol{k} \times \boldsymbol{n}$ (T_3) and $(-\mu F\cos\theta\cos\psi_s)\boldsymbol{m}$ (T_4). T_3 produces an angular velocity

$$(d\theta/dt)_F = \left(D_i \alpha \cos\theta \sum_s \sin\psi_s\right) k \times n \qquad (A11)$$

for the aggregate when summed over all monomers. T_4 can be further split up into $([\mu F\cos\theta/\tan\theta]$ $\cos\psi_s)\boldsymbol{n}$ (T_5) and a torque T_6 parallel to $\boldsymbol{k}$ (see fig. 8a). T_6 is ineffective in changing the γ_i function since it rotates the whole aggregate about the field direction k, but T_5, again summed over the aggregate, results in an additional

$$(d\psi_s/dt)_F = \left(D_i \frac{\alpha\cos^2\theta}{\sin\theta} \sum_s \cos\psi_s\right) n \qquad (A12)$$

for each molecule (to be added to that in (A10)).

The net influx into $d\Omega$ because of rotational diffusion can be derived in strict analogy to (A8) if the respective diffusional fluxes j'_θ and j'_s are known. The θ-flux is easily seen to be

$$j'_\theta = -D_i \, \partial\gamma_i/\partial\theta, \qquad (A13)$$

while the other fluxes may depend in a more complicated way on the gradient of γ_i. In general

$$j'_s = -\sum_\sigma D_{s\sigma} \, \partial\gamma_i/\partial\psi_\sigma, \qquad (A14)$$

where the rotational diffusion coefficients $D_{s\sigma}$ can be determined from the fact that at equilibrium $\bar{\gamma}_i$ is given by the Boltzmann distribution in (A4) and $(\partial\gamma/\partial t)_F = -(\partial\gamma/\partial t)_D$. This yields

$$D_{ss} = D_i \cos^2\theta/\sin^2\theta + D_n \qquad (A15)$$

and

$$D_{s\sigma} = D_i \cos^2\theta/\sin^2\theta \quad (s \neq \sigma). \tag{A16}$$

Now substituting for j_θ and j_s in $(\partial\gamma/\partial t)_F$ as given by (A8), using (A9–12), and similarly for j'_θ and j'_s in $(\partial\gamma/\partial t)_D$, using (A13–16), the general equation of continuity

$$\partial\gamma_i/\partial t = (\partial\gamma_i/\partial t)_D + (\partial\gamma_i/\partial t)_F \tag{A17}$$

may be expressed in the form (where $\alpha = \mu F/kT$)

$$\frac{\partial\gamma}{\partial t} = -\frac{1}{\sin\theta}\left[\frac{\partial}{\partial\theta}\left(\sin\theta \cdot \gamma_i D_i \alpha \cos\theta \sum_s \sin\psi_s\right)\right.$$
$$+ \sum_s \frac{\partial}{\partial\psi_s}\left(\sin\theta \cdot \gamma_i\left(D_n \alpha \sin\theta \cos\psi_s\right.\right.$$
$$\left.\left.\left. + D_i \frac{\alpha\cos^2\theta}{\sin\theta}\sum_\sigma \cos\psi_\sigma\right)\right)\right]$$
$$+ \frac{D_i}{\sin\theta}\frac{\partial}{\partial\theta}\left(\sin\theta\frac{\partial\gamma_i}{\partial\theta}\right) + D_i\frac{\cos^2\theta}{\sin^2\theta}\sum_{s\sigma}\frac{\partial^2\gamma_i}{\partial\psi_s\partial\psi_\sigma}$$
$$+ D_n\sum_s\frac{\partial^2\gamma_i}{\partial\psi_s^2}. \tag{A18}$$

With a small alternating field $F = F_0\exp(j\omega t)$ applied (if α_0^2 terms are neglected, since $\alpha_0 = \mu F_0/kT \ll 1$)

$$\gamma_i = \gamma_i^0\left(1 + \frac{\alpha_0\exp(j\omega t)}{1 + j\omega\tau_i}\sin\theta\sum_s\sin\psi_s\right) \tag{A19}$$

is found to be the appropriate solution of (A18), giving a relaxation time

$$\tau_i = 1/(D_i + D_n). \tag{A20}$$

Finally, substituting for γ_i in (A3)

$$P_i = \frac{\bar{P}_i\exp(j\omega t)}{1 + j\omega\tau_i} \tag{A21}$$

yielding eq. (6) in the text.

References

[1] K.E. van Holde and G.P. Rossetti, Biochem. 6 (1967) 2189.
[2] A.D. Broom, M.P. Schweizer and P.O.P. Ts'o, J. Amer. Chem. Soc. 89 (1967) 3612.
[3] K.E. van Holde, G.P. Rossetti and R.D. Dyson, Ann. N.Y. Acad. Sci. 164 (1969) 279.
[4] R. Bretz, A. Lustig and G. Schwarz, Biophys. Chem. 1 (1974) 237.
[5] P.O.P. Ts'o, in: Basic principles in nucleic acid chemistry, vol. I, ed. P.O.P. Ts'o (Academic Press, New York, 1974).
[6] D. Pörschke and F. Eggers, Eur. J. Biochem. 26 (1972) 490.
[7] V.A. Bloomfield, D.M. Crothers and I. Tinoco Jr., Physical chemistry of nucleic acids (Harper and Row, New York, 1974).
[8] H. Berthod and B. Pullmann, Biochem. and Biophys. Res. Commun. 46 (1972) 125.
[9] H.F. Eicke and J.C.W. Shepherd, Helv. Chim. Acta 57 (1974) 1951.
[10] C.P. Lawinski, J.C.W. Shepherd and E.H. Grant, J. of Microwave Power 10 (1975) 147.
[11] J.C.W. Shepherd and E.H. Grant, Proc. Roy. Soc. A 307 (1968) 335.
[12] J.G. Kirkwood, in: Proteins, aminoacids and peptides, ed. E.J. Cohn and J.T. Edsall (Reinhold, New York, 1943).
[13] A. Budó, Physik. Zeits. 39 (1938) 706.
[14] J. Perrin, Compt. Rend. Acad. Sci. 149 (1909) 549.
[15] H. de Voe and I. Tinoco Jr., J. Mol. Biol. 4 (1962) 500.
[16] A. Budó, J. Chem. Phys. 17 (1949) 686.
[17] O. Sinanoğlu and S. Abdulnar, Fed. Proc. 24 (1965) Suppl. 15, S-12.
[18] G. Schwarz, J. Phys. Chem. 71 (1967) 4021.
[19] M.P. Heyn, C. Nicola and G. Schwarz, J. Phys. Chem., submitted.